Associating brain topological networks to cognitive performance.

Fabrizio Parente* and Alfredo Colosimo*

*Dept. of Anatomy Histology Forensic Medicine and Orthopaedics , Sapienza University of Rome

Abstract

Recent applications of graph theory to brain networks showed the possibility of a relation between network topological indexes and cognitive abilities. In this paper we want to study the relation between the topology of brain networks and a known parameter of executive functions, such as perseveration, using the WCST. To this end, nine healthy subjects were subjected to a fMRI acquisitions with a 3 Tesla Siemens scanner under condition of resting state and evaluated with the WCST. The images were analyzed using the following Matlab toolboxes: SPM8 and Functional Connectivity Toolbox. From WCST data the indexes of perseverative, nonperseverative errors and perseverative response were calculated. A small-world feature appears in the cost range (T) 0.45 - 0.50: In this interval, the γ index shows a positive correlation with perseverative responses (T=0.50, r=0.864, p=0.006). Moreover, among the γ values of single cerebral regions (T=0.50), the middle part of orbital frontal gyrus left (r=0.920, p=0.001) show a significant trend for positive correlation with perseverative responses. These results suggest a relation between network's segregation and perseveration; more specifically a greater segregation of subnetworks is related to a lower adaptability of behavior to the environment changes. Our findings can provide hints to understand the pathological alterations of mental disease related to impairment of executive functions.

Keywords. fMRI, Resting state, Executive functions, WCST, Graph theory

Contents

Abbreviations used in the text:

fMRI: Functional magnetic resonance imaging
BOLD: Blood oxygenation level dependent
ROI: Region of interest
IQ: Intelligence quotient
WCST: Wisconsin card sorting test
SPM: Statistical Parametric Mapping
AM: Adjacency matrix
C: Clusterig coefficient
L: Characteristic Short Path Lenght
k: Node degree
E: Global efficiency
E_{loc}: Local efficienct
γ: Gamma value
λ: Lambda value
S: Small-worldess
T: Threshold cost

1 Introduction.

In task-related fMRI technique, the performance of cognitive tests is thought to influence the activation of one or more specific cerebral areas. With different analysis techniques it is possible to integrate these cerebral areas into a different networks. As a matter of fact, BOLD signal fluctuations of these areas have been observed as correlated between each other in the resting state [1], such correlations remain stable even in the lack of given stimuli and involve a relevant fraction of brain metabolism. The observed correlation pattern is reminding the more general time dependent correlation between two spatially distributed neurophysiological events called *functional connectivity*. In such a frame, the set of these stable functional connections in the absence of specific stimulation are defined *neurocognitive networks* (Figure 1).

In this contest, *the graph theory* [2] provides a theoretical support in the investigation of complex network topologies [3, 4] (for details see Appendix 1) allowing us to answer critical questions on brain networks like: 1) How is the topology of brain network organized? 2) How efficiently the brain integrates the information coming from subnetworks? A key concept of this approach is the identification of a *"small-world"* architecture [5, 6] of brain network, indicating the possible existence of an intermediate state between maximal segregation and maximal integration of network's nodes. Recent investigations found some significant correlations between the functional efficiency level of the network and cognitive indexes [7–10], indicating a possible dependence between cognitive abilities and topological features of brain networks.

An important cognitive ability, also for clinical implication for neurologic and psychiatric diseases, are the executive functions. A recent definition of executive functions has been given by Funahashi: "a product of the coordinated operation of various processes to accomplish a particular goal in a flexible manner" [11]. Thus, mental flexibility assumes an important role for the realization of this ability and can be objectively measured by means of the classical Wisconsin Card Sorting Test (WCST, see Appendix 2). In such a context, the using of WCST initially showed an altered performance in patients with prefrontal cortex lesions [12]. More recently, the using of task-related fMRI methodology showed an unclear picture with distributed activations in frontal and nonfrontal regions [13–20]. For an exhaustive re-

view of such intricate situation see [21].

From the bulk of the above mentioned results a complex picture appears, in which distributed brain networks are involved in the WCST performance. Complex network approach can be suggested as an approach to distinguish cognitive functions which depend upon large brain network, from other cognitive functions depending upon more localized brain network clusters. Assuming that cognitive function of the first type would be more depending upon a higher communication level, while the other type would be more depending upon the clustering of specific subnetworks, the two types could reach an equilibrium state between segregation and integration forces to be ultimately identified as a small-world state. In order to validate this hypothesis we adopt the following strategy:

- Studying the functional brain network in healthy subjects looking at integration and segregation features.
- Studying the relation between brain network features and cognitive performance.
- Exploring the relation between specific areas within more distributed brain network and cognitive performance.

2 Materials and methods.

2.1 Participants and data collection.

Nine volunteers were selected for negative anamnesis of neurological and psychiatric diseases. Among these, six were females, the mean age was 27.9 years (with minimum and maximum 20 and 42 respectively) and average school attendance 14.1 years (7 subjects with 13 years and 2 with 18). All the participants were subjected to an ecoplanar sequence (EPI) in a resting state condition using a Siemens MRI 3 Tesla, in the Department of Neurological Sciences, Sapienza - University of Rome. fMRI images were collected under the following conditions: TR= 3000ms; TE= 30ms; 40 slices; thickness 4 mm; voxels dimension 3.8x 3.8 x 4; scans 150; see Figure 2. During the scanning time the volunteers were recommended to keep their eyes closed and think

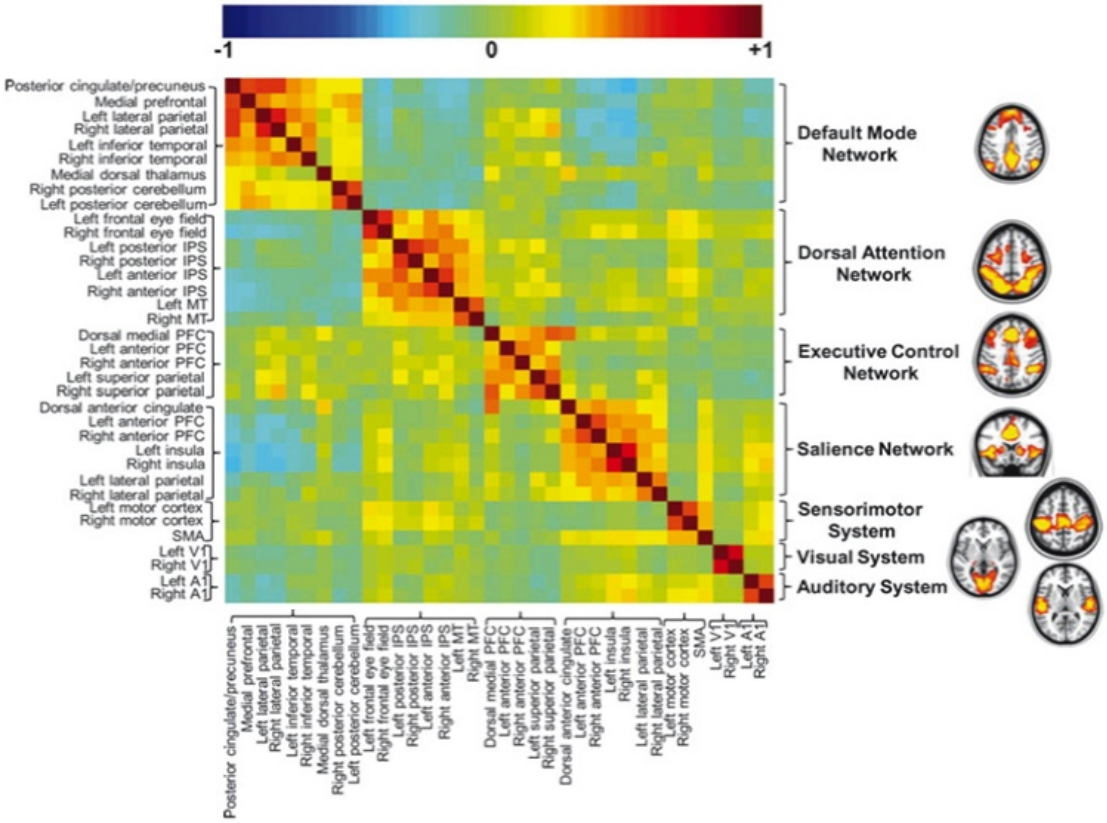

Figure 1: *Correlation matrix of BOLD signals' from different anatomical regions.* Functional grouping of anatomical regions provided by [22] on the basis of fMRI data.

of nothing in particular without falling asleep. Before the scanning all the subjects signed the informative consensus document.

2.2 fMRI data preprocessing.

DICOM images were converted to the *spm analyze* format by *MRI-converter*. For image preprocessing the following Matlab toolboxes were used: *SPM8* (Statistical Parametric Mapping, Wellcome Department of Cognitive Neurology, London, UK) and *Functional Connectivity Toolbox*. In all cases the first 10 images were discarded, the remaining were reoriented to the 10 scanning volume, corrected for the acquisition time, realigned and spatially normalized on the reference standard template in order to reduce the individual anatom-

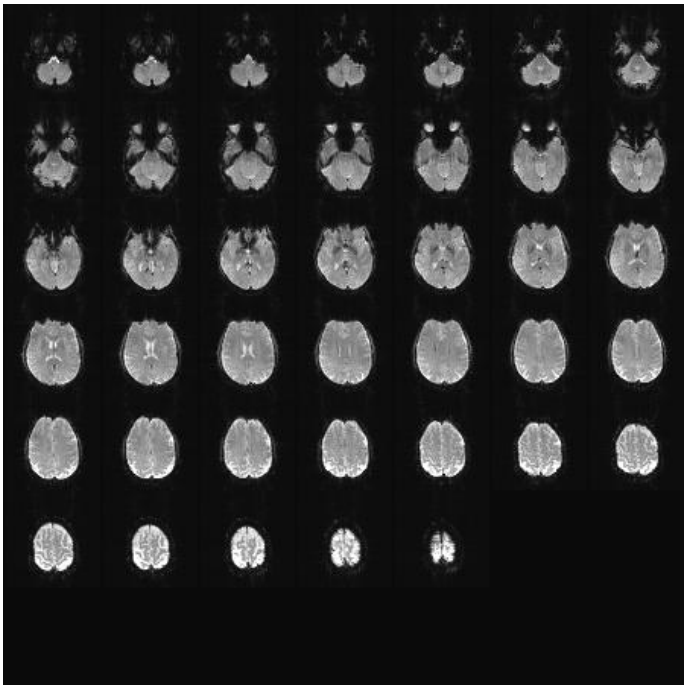

Figure 2: *Slices from a single subject in a typical fMRI session (raw data, see the text for details).*

ical variability. As standard template an EPI image was used with reference coordinate from Montreal Neurological Institute (MNI). Subsequently, the images were corrected for noise source from cephalorachidian liquid, white matter signal, grey matter signals and body movements.Finally, a band-pass filter was utilized in the range of 0.008-0.09 Hz on BOLD signals.

2.3 fMRI data analysis.

Our analytical strategy can be schematized as follows (Figure 3):

- The images of subjects were divided into 90 ROI by automatic anatomical labeling [23].
- From each ROI the time series were extracted for each subject (acquisition time 450 sec with 3 Hz frequency, in order to obtain discrete series of 150 units. After excluding the first 10 images, as above described, 140 units were left for analysis.)

- For each subject a correlation matrix was calculated for all possible couples of the 90 ROIs. This information was used as a functional connectivity index, (Figure 4).

- A proportional threshold T (cost, see appendix 1) was applied to the previous matrices. Such a threshold was used to select the fraction of links with higher correlation coefficient on the matrix correlation, in order to characterize, within the original network, possible subnetworks of increasing size. To this purpose, the networks with T from 0.05 to 0.5, at 0.05 intervals, were studied and each network obtained was binarized. Finally, the associated random network of each binarized network was calculated preserving the node degree distribution of the original network (20 iterations for node re-wiring).

- For each threshold range and related random network the following indexes were calculated: C, L, γ, λ and S (for a detailed description of the above indexes see Appendix 1). From the T where all the networks are fully connected (not a node without link exists in the networks of subjects) the U Mann-Whitney test was used for each threshold in order to find the small-world range, namely C of random networks significantly lower than the real networks and no difference between L of real networks and random networks.

- The correlation matrix of each subject was submitted to the proportional threshold corresponding to the small-world condition and the following indexes were calculated: C, L, k, E, E_{loc}, γ, λ and S.

2.4 Neuropsychological evaluation.

After imaging acquisition the WCST was administered to each subject in a computerized version on the PEBL (The Psychology Experiment Building Language, http://pebl.sourceforge.net/) platform. Then, the results were imported in an Excel file for the task performance analysis and the following behavioral indexes were calculated : perseverative errors, nonperseverative errors and perseverative responses (see appendix 2).

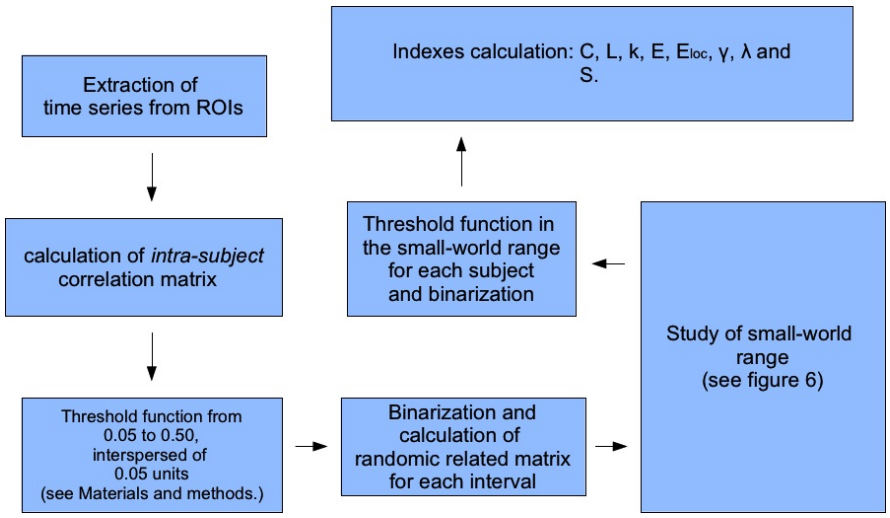

Figure 3: flowchart of the data analysis methods.

2.5 Statistical analysis.

The following statistical analyses were made: partial correlations (controlling variable = age) between behavioral data and network indexes. In particular, a number of performance descriptors, namely the rate of perseverative responses, perseverative errors and nonperseverative errors, were correlated with the following network indexes: γ and λ. Finally, the same statistical analysis was performed on γ value of each node and perseverative responses. In addition, for controlling demographic variables, such as gender and school attendance, a series of U Mann-Whitney test were made on the groups male-female and high school graduation(13 years)-university degree(18 years), for both behavioral data and network indexes. All the the analyses were carried out by the IBM SPSS version 20.

3 Results.

3.1 Behavioural data.

Our results on behavioral data include: average rate of perseverative error (18.51, maximum and minimum values respectively 8.03 - 33.59); average rate of nonperseverative error (10.51, 4.69 - 23.44); average rate of perseverative responses (39.26, 31.25 - 57.03) see also Figure 5. Nonsignificant gender or school attendance differences were detected by U Mann-Whitney test.

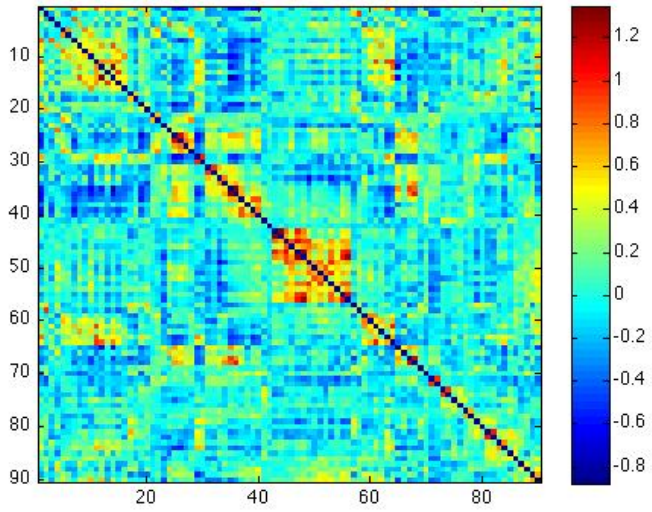

Figure 4: *Correlation Matrix between ROIs of a single subject from fMRI data.* The raw data are plotted in a normalized, false color scale.

3.2 Description of brain complex network model.

Following the procedure detailed in the methods section, a fully connected network appears starting from a cost value = 0.15. From such a value and up to 0.50, looking for a threshold range able to induce the smallworld state, the trend of the following indexes was studied: C, L, γ, λ and S, (see Figure 6). U Mann-Whitney test was used to determine the differences between random networks and original networks: C average of original networks remains higher as compared to its equivalent of randomized networks in all cases (p=0.0000411 one tail), while L average becomes closer and closer to the corresponding randomic value up to the point where the indexes coalesce (T=0.45, p=0.050 one tail; T=0.50, p=0.050 one tail; T<0.45, p=0.0000411 one tail). Moreover, (not shown in the figure) λ becomes equal to 1.0003 at T=0.45, while γ and S remain above 1.20 up to all T values. Hence, the smallworld interval was chosen between 0.45 and 0.50 units. In a further step, such threshold values were applied to each subject matrix and the relative mean values collected in Table 1. Nonsignificant differences between genders or school attendance were detected by the U Mann-Whitney test.

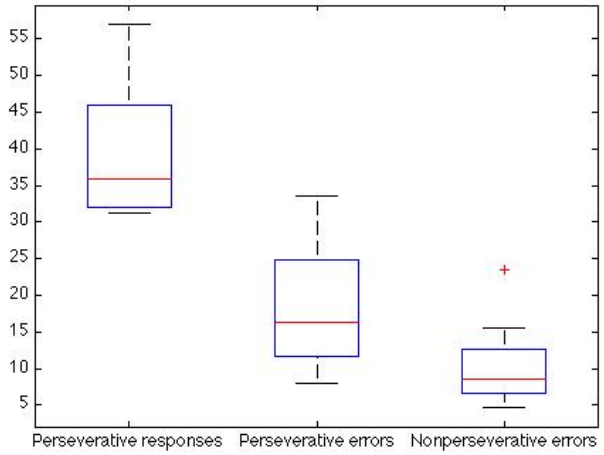

Figure 5: *Box-plot of behavioural performance of 9 normal subjects (red line is the median). See the text for actual numerical values*

Table 1: *Network Descriptors used in this work.*

cost	0.45	0.50
C	0.6034 (0.591 - 0.628)	0.629 (0.615 - 0.651)
L	1.380 (1.379 - 1.381)	1.333 (1.333 - 1.334)
E_{loc}	0.803 (0.797 - 0.818)	0.816 (0.810 - 0.828)
E	0.725 (0.724 - 0.725)	0.750 (0.750 - 0.750)
k	40.056	44.500
γ	1.269 (1.236 - 1.322)	1.200 (1.178 - 1.235)
λ	1.000 (0.999 - 1.001)	1.000 (0.999 - 1.000)
S	1.268 (1.235 - 1.321)	1.200 (1.178 - 1.235)

3.3 Global network properties and executive functions.

Partial correlations were used in statistical analysis for taking into account the influence of subjects age, the correlated variables are γ and λ indexes with perseverative, nonperseverative errors and perseverative responses. The results show a positive correlation of perseverative responses and errors with γ for multiple comparison uncorrected p-value. After Bonferroni correction there is a trend in γ value of 0.50 threshold and perseverative responses. No significant correlations were obtained with nonperseverative errors (see Table 2).

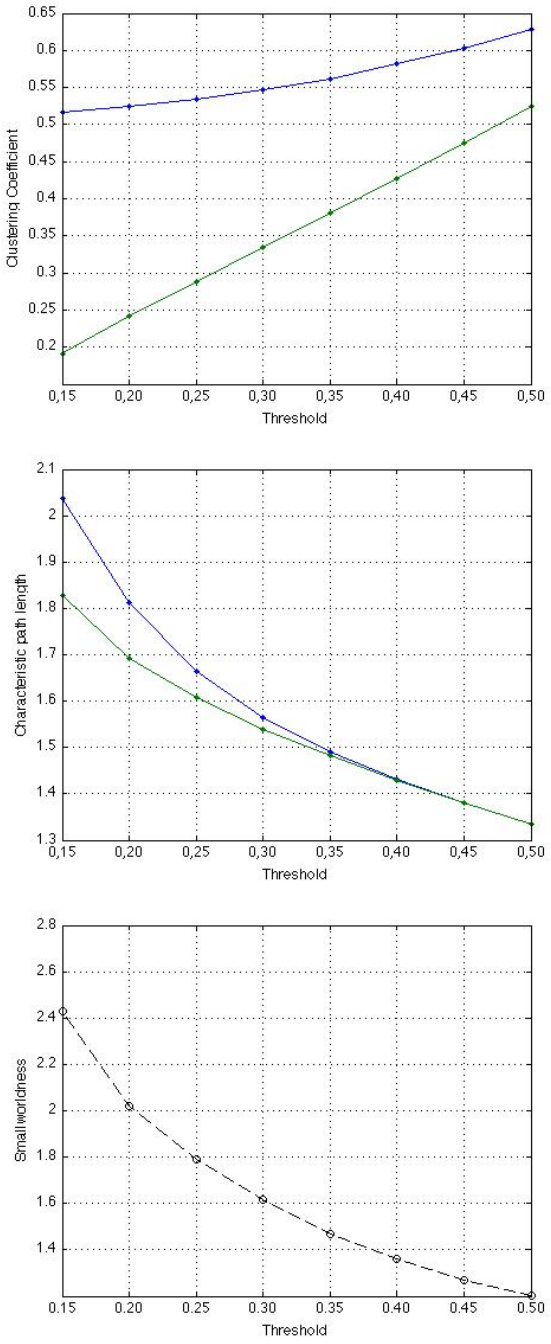

Figure 6: Top, middle and bottom panels contains, respectively: the cost dependence of clustering coefficient (blue curve), average path lenght (blue curve) and smallworldness index. The top and middle panels also include the randomized network elements (green curve) as a reference.

Table 2: Correlation between behavioral data and indexes of graph at different threshold of T.

Errors Type	Index	0.45	0.50
Perseverative errors	Gamma	r=0.701, p=0.053	r=0.736, p=0.037*
	Lambda	r=0.317, p=0.444	r=-0.142, p=0.737
Nonperseverative errors	Gamma	r=0.275, p=0.509	r=0.170, p=0.688
	Lambda	r=-0.503, p=0.204	r=0.086, p=0.839
Perseverative responses	Gamma	r=0.787, p=0.020*	r=0.864, p=0.006**
	Lambda	r=0.356, p=0.387	r=0.120, p=0.777

3.4 Local network properties and executive functions.

The above partial correlation analysis was carried out also for node features at the threshold 0.50. In particular between γ of each node and perseverative responses.

Table 3: Correlation between γ value of each node and perseverative responses.

ROI	Perseverative responses
Precentral gyrus left	r=0.882, p=0.004
Rolandic operculum right	r=0.743, p=0.035
Supplementary motor area left	r=0.799, p=0.017
Medial part of superior frontal gyrus right	r=0.725, p=0.042
Middle part of orbital frontal gyrus left	r=0.920, p=0.001
Inferior parietal lobule right	r=-0.849, p=0.008
Inferior parietal lobule left	r=-0.738, p=0.037

In table 3 were inserted the brain regions that show a significant correlations between their γ value and perseverative responses, uncorrected for multiple comparision. Moreover, no correlation remains significant after Bonferroni correction for multiple comparisons, but there is a significant trend in one region such as middle part of left orbital frontal gyrus (Figure 7).

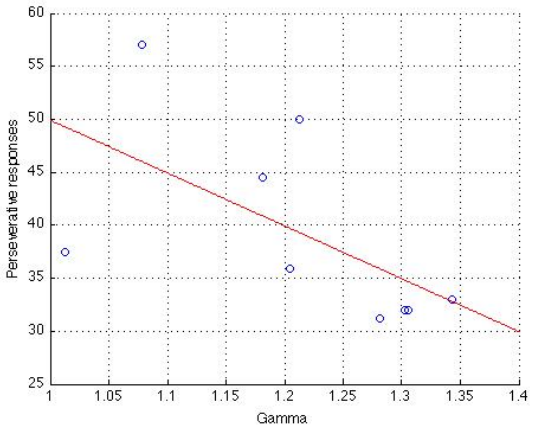

Figure 7: Scatter plot of perseverative responses and middle part of left orbital frontal gyrus.

4 Discussion.

4.1 Brain networks and smallworld networks.

Graph theory as applied to brain connectivity maps allows uncovering their emergent properties and leads, hopefully, to a better understanding of the *brain system*. In particular, such a tool enlights the integration-segregation features of brain network. For an optimal working, not only some well defined brain structural modules are needed, but also an efficient functional integration between them. The small-word architecture, as quantified by the smallworldness index (S), clearly points to such a conclusion, since it defines an equilibrium between the segregation features of lattice-like graphs and the integration features typical of randomic networks (see Appendix 1).

A smallworldness » 1 is considered an indication of reliable segregation-integration equilibrium [24]. Under our conditions such a value has been obtained within a 0.45 - 0.50 window of the *cost function*. The easiest interpretation of the *cost function* (see Appendix 1), in this context, refers to the energy supply limitations unavoidable with the increasing number of connections [25].

4.2 Executive functions and global neural network.

A major question we would like to address here, concerns the connection between the results of the WCST with the segregation level of specific subnetworks or the integration of whole brain network. It should be mentioned, however, that the main use of the WCST [12] has been made, up to now, in the study of executive functions. In our analysis the test results have been represented in the form of perseveratove responses, perseverative and nonperseverative errors, in the aim to distinguish between their random or specific causes.

Our results indicate that perseverative responses show a slightly positive correlation with the γ index, and no correlation with the λ index, at the highest considered cost threshold. This means that the probability of making perseverative responses increases when increasing segregation of the network. Similar results were reached by other approaches based of the IQ index as a behavioural parameter. For instance, Van de Heuvel et al. [7], using as nodes single voxels, showed a negative correlation between the λ and the total IQ index. In addition, Song et al. [10], using as nodes the default network ROIs, put in evidence a significant difference in the L and E indexes between two groups of different QI, pointing to a shorter path length for subjects with higher IQ. Such conclusions seem confirmed by the analysis of anatomical connectivity data by means of DTI [8].

In conclusion, the previously mentioned results indicate a correlation between IQ and integration of whole brain network, allowing to estimate the former one through a quantitative parameter. On the basis of our results, we hypothesize that it is possible also with others and more particular cognitive abilities such executive functions. As a matter of fact, only in a single case [9] it has been estimated the correlation of a well defined cognitive abilities (working memory) with a network index (modularity), which could be interpreted as a correlation with a segregation level.

4.3 Executive functions and local neural networks.

In order to better estimate the driving forces underlying the global correlation between cerebral segregation and perseverative responses, we focused on the γ index of each node in the brain network.

This analysis shows results in line with global network analysis. In particular, the middle part of the left orbital frontal gyrus shows positive correlation with trend toward significance. This cerebral area has been associated already to WCST in previous fMRI studies [13–15, 18–20] which confirms the importance of the prefrontal region in the performance of task-shift function of the executive functions. In addition, the γ value used in the analysis gives additional information on the fact that this region uses the transfer of information between the networks: in fact, a decrease in this index indicates a lower degree of functional communication of that region in its sub-network and an increase with the remaining. We can speculate that this node may have an important role in communication between their neighboring nodes, belonging to others sub-networks, to improve the adaptation of behavior to the environment changes.

5 Conclusions.

It seems fair to suggest that our results confirm a dependence between the properties of the brain network and behavioral indices already found for the IQ. In this frame, the results show that in order to facilitate mental flexibility there is a greater importance of the specific integration between different brain sub-networks. Besides than opening some new questions over the role of brain mechanisms in the control of executive functions, our findings also provide some hints to understand the mechanisms of extremely severe pathological alterations. For instance, in the case of schizophrenia, an appropriate index of mental flexibility, more than indicating a defective functioning of specific regions, could point to a distributed brain malfunctions that impair the functional connectivity between different regions, and hence alter the topology of their network.

References

[1] Raichle M.E., MacLeod A.M., Snyder A.Z., Powers W.J., Gusnard D.A., and Shulman G.L. A default mode of brain function. *Proceedings of National Academy of Science of the United States of America*, 14:180–190, 2010. 5

[2] Boccaletti S., Latora V., Moreno Y., Chavez M., and Hwang D.-U. Complex networks: Structure and dynamics. *Physics Reports*, 424:175–308, 2006. 5

[3] Bullmore E and Sporns O. Complex brain networks: graph theoretical analysis of structural and functional systems. *Nat Rev Neurosci.*, 10(3):186–98, 2009. 5

[4] Rubinov M. and Sporns O. Complex network measures of brain connectivity: uses and interpretations. *Neuroimage.*, 53(3):1059–69, 2009. 5, 22

[5] Achard S., Salvador R., Whitcher B., Suckling J., and Bullmore E. A resilient, low-frequency, small-world human brain functional network with highly connected association cortical hubs. *J. Neurosci.*, 26(1):63–72, 2006. 5

[6] Achard S. and Bullmore E. Efficiency and cost of economical brain functional networks. *PLoS Comput. Biol.*, 3(2):e17, 2007. 5

[7] Van den Heuvel M.P., Stam C.J., Kahn R.S., and Hulshoff Pol H.E. Efficiency of functional brain networks and intellectual performance. *J. Neurosci.*, 29(23):7619–7624, 2009. 5, 16

[8] Li Y., Liu Y., Li J., Qin W., Li K., Yu C., and Jiang T. Brain anatomical network and intelligence. *PLoS Comput. Biol.*, 5(5):e1000395, 2009. 5, 16

[9] Stevens A.A., Tappon S.C., Garg A., and Fair D.A. Functional brain network modularity captures inter- and intra-individual variation in working memory capacity. *PLoS One*, 7(1):e30468, 2012. 5, 16

[10] Song M., Zhou Y., Li J., Liu Y., Tian L., Yu C., and Jiang T. Brain spontaneous functional connectivity and intelligence. *Neuroimage*, 41(3):1168–1176, 2008. 5, 16

[11] Funahashi S. Neuronal mechanisms of executive control by the prefrontal cortex. *Neurosci Res.*, 39(2):147–65, 2001. 5

[12] Eling P., Derckx K., and Maes R. On the historical and conceptual background of the wisconsin card sorting test. *Brain Cogn.*, 67(3):247–53, 2008. 5, 16

[13] Volz H. P., Gaser C.and Hager F., Rzanny R., Mentzel H. J., Kreitschmann-Andermahr I., and et al. Brain activation during cognitive stimulation with the wisconsin card sorting test Ð a functional mri study on healthy volunteers and schizophrenics. *Psychiatry Research.*, 75:145–157, 1997. 5, 17

[14] Monchi O., Petrides M., Petre V., Worsley K., and Dagher A. Wisconsin card sorting revisited: Distinct neural circuits participating in different stages of the task identified by event-related functional magnetic resonance imaging. *The Journal of Neuroscience*, 21:7733–7741, 2001. 5, 17

[15] Lie C. H., Specht K., Marshall J. C., and Fink G. R. Using fmri to decompose the neural processes underlying the wisconsin card sorting test. *Neuroimage*, 30:1038–1049, 2006. 5, 17

[16] Mentzel H. J., Gaser C., Volz H. P., Rzanny R., Hager F., Sauer H., and et al. Cognitive stimulation with the wisconsin card sorting test: Functional mr imaging at 1.5 t. *Radiology.*, 207:399–404, 1998. 5

[17] Konishi S., Nakajima K., Uchida I., Kameyama M., Nakahara K., Sekihara K., and et al. Transient activation of inferior prefrontal cortex during cognitive set shifting. *Nature Neuroscience.*, 1:80Ð84, 1998. 5

[18] Konishi S., Kawazu M., Uchida I., Kikyo H., Asakura I., and Miyashita Y. Contribution of working memory to transient activation in human inferior prefrontal cortex during performance of the wisconsin card sorting test. *Cerebral Cortex.*, 9:745–7533, 1999. 5, 17

[19] Konishi S., Hayashi T., Uchida I., H. Kikyo, Takahashi E., and Miyashita Y. Hemispheric asymmetry in human lateral prefrontal cortex during cognitive set shifting. *Proceedings of the National Academy of Sciences of the United States of America.*, 99:7803Ð7808, 2002. 5, 17

[20] Konishi S., Jimura K., Asari T., and Miyashita Y. Transient activation of superior prefrontal cortex during inhibition of cognitive set. *The Journal of Neuroscience.*, 23:7776–7782, 2003. 5, 17

[21] Nyhus E. and Barceló F. On the historical and conceptual background of the wisconsin card sorting test. *Brain Cogn.*, 71(3):437–51, 2003. 6

[22] Raichle M. E. The restless brain. *BRAIN CONNECTIVITY*, 1:3–12, 2011. 7

[23] Tzourio-Mazoyer N., Landeau B., Papathanassiou D., Crivello F., Etard O., Delcroix N., Mazoyer B., and Joliot M. Automated anatomical labeling of activations in spm using a macroscopic anatomical parcellation of the mni mri single-subject brain. *NeuroImage*, 15(1):273Ð289, 2002. 8

[24] Humphries M.D. and Gurney K. Network 'small-world-ness': a quantitative method for determining canonical network equivalence. *PLoS One*, 3(4):e0002051, 2008. 15

[25] Bullmore E. and Sporns O. The economy of brain network organization. *Nature Reviews Neuroscience*, page doi:10.1038/nrn3214, 2012. 15

[26] Bullmore E. and Bassett S. Brain graphs: Graphical models of the human brain connectome. *Annu. Rev. Clin. Psychol.*, 7:113Ð40, 2011. 21

[27] Latora V. and Marchiori M. Efficient behavior of small-world networks. *Phys Rev Lett.*, 87(19):198701, 2001. 21

[28] Newman M.E.J. Modularity and community structure in networks. *Proc. Natl. Acad. Sci. U. S. A.*, 103:8577–8582, 2006. 21

[29] Watts D.J. and Strogatz S.H. Collective dynamics of small-world networks. *Nature*, 393:440–442, 1998. 22

6 Appendix 1: Graph theory.

According to the graph theory, a network is defined as an ensemble of N nodes linked by K edges. Three different types of networks may be distinguished, whether links are i) directed, ii) weighted, or iii) binarized. In what follows we deal with binary networks, within which links are not endowed with weight or direction, and may only exist (1) or non exist (0). The binary values may be arranged in an NxN squared matrix, called the Adiacency Matrix (AM), where the i,j location indicates the (non)existence of a link between i and j nodes. In fMRI studies the links are defined in terms of functional connectivity between nodes corresponding to ROIs localized in specific voxels [26]. From the AM is straightforward calculate the following indices of graph's description:

- C = *Clustering Coefficient* (index of segregation);
- L = *Characteristic Path Length* (index of integration);

By consideration of the two above indexes, the following graph typologies can be distinguished:

- *regular* or *lattice-like* type: high C and high L;
- *random* type: low L and low C;
- *small-world* type: intermediate C and L (Figure 8);
- *scale-free* type: low level of L and intermediate C between *random* and *small-world* types (power law distribution of Node Degrees)

In addition, two other indexes have been proposed to characterize the network topology, namely: *Global* and *Local Efficiency* [27], appropriate for estimating the communication level between nodes in whole network and in subnetworks respectively; and the *Modularity* index, indicating the clear presence of subnetworks [28] .

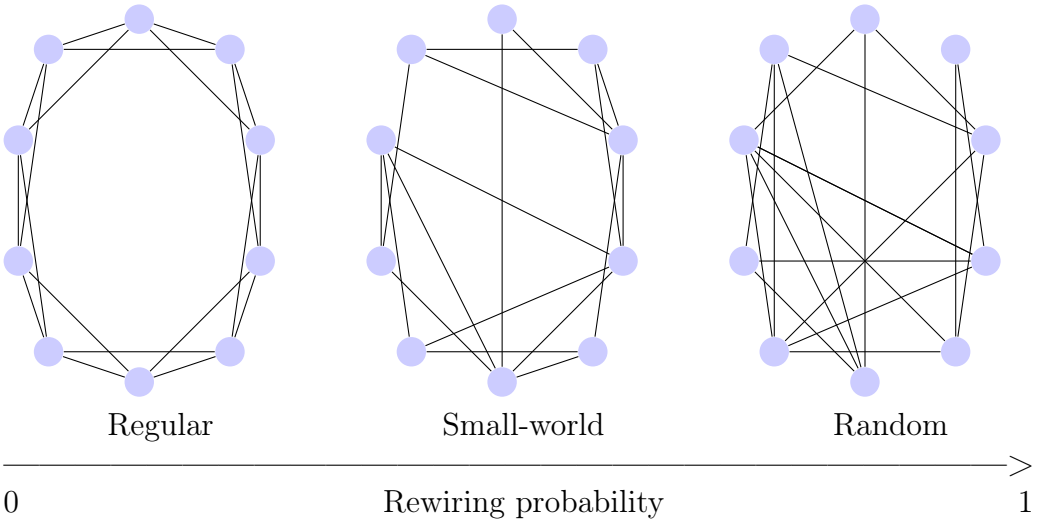

Figure 8: Intermediate location of Smallwordness in the Regular → Random transition of network as a function of links rewiring. (From [29]). Rewiring probability is the probability of any edge to be rewired into the graph as a random edge.

6.1 Network parameters.

The Graph Theory indexes [4], used in the present contribution are listed below:
- N = total number of nodes in the network.
- L = total number of links in the network.
- (i,j) = is a link between i and j nodes.
- a_{ij} = link value between nodes i and j (= 0/1 in binary networks).

Degree: Number of links in node i.

$$k_i = \sum_{j \in N} a_{ij} \tag{1}$$

Shortest Path Length: Minimal Number of Links connecting two nodes i and j, corresponding to the distance between them.

$$d_{ij} = \sum_{a_{uv} \in g_i \leftrightarrow_j} a_{uv} \tag{2}$$

where $g_i \leftrightarrow_j$ is the Shortest Path passing through u and v intermediate nodes of the total trajectory between i and j.

Clustering Coefficient: the fraction of node neighbors that are neighbors of each other.

$$C = \frac{1}{N} \sum_{i \in N} \frac{\sum_{j,h \in N} a_{ij} a_{ih} a_{jh}}{k_i (k_i - 1)} \tag{3}$$

Characteristic Short Path Lenght: Average of Short Path Length.

$$L = \frac{1}{N} \sum_{i \in N} \frac{\sum_{j \in N, i \neq j} d_{ij}}{N - 1} \tag{4}$$

Cost: Connectivity Index.

$$0 \leq k = \frac{2 * \epsilon_\tau}{N(N-1)} \leq 1 \tag{5}$$

where ϵ_τ is the number of links associated to a given (τ) threshold.

Global Efficiency: Integration level between nodes, inversely related to L.

$$E = \frac{1}{N} \sum_{i \in N} \frac{\sum_{j \in N, i \neq j} d_{ij}^{-1}}{N - 1} \tag{6}$$

Local Efficiency: Segregation Level (related to C).

$$E_{loc} = \frac{1}{N} \sum_{i \in N} \frac{\sum_{j,h \in N, j \neq i} a_{ij} a_{ih} [d_{jh}(N_i)]^{-1}}{k_i (k_i - 1)} \tag{7}$$

with $d_{jh}(N_i)$ is the length of the shortest path between j and h, that contains only neighbors of i.

Gamma : C of a network normalized to the corresponding random network ($\gamma > 1$ in the *small world* networks).

$$\gamma = \frac{C}{C_{rand}} \tag{8}$$

Lambda: L of a network normalized to the corresponding random network (about 1 in the *small world* networks).

$$\lambda = \frac{L}{L_{rand}} \tag{9}$$

Small-Worldness: $S > 1$ in *Small World* networks.

$$S = \frac{C/C_{rand}}{L/L_{rand}} \tag{10}$$

7 Appendix 2: Wisconsin Sorting Task.

The Wisconsin Sorting Task was originally developed by Grant and Berg to estimate the abstract reasoning and the adaptation to an abrupt change of the response strategy. This task was successively modified by B. Milner to evaluate alterations consequent to prefrontal lesions. In the classical protocol, the task consists in the association between one of *128 response cards* with one of *four key cards*. The cards are distinguishable by the color, shape and number of represented objects. An initial association can be modified in subsequent steps, as a result of the experimenter's feedback. After 10 consecutive correct associations, on the basis of one of the three above listed features, the association rule changes by choosing a different feature. The test is over after 128 responses or after 10 correct responses in six feature changes (60 total correct responses) (Figure 9). In such a context errors are connected to inability to recognize the current rule. In particular, if errors consist in the failing recognition of the rule updating then are defined as "perseverative" errors, else if the response fall in a card of the previous rule without falling in error then are defined as perseverative responses. Perseverative, nonperseverative errors and perseverative responses quantitatively estimated, are used as performance indicator in the WCST.

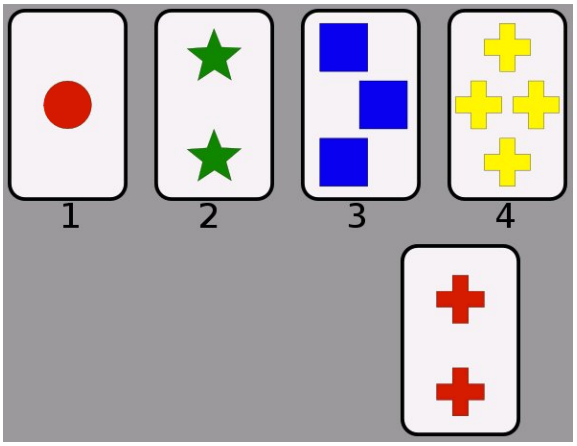

Figure 9: WCST carried out on the PEBL platform. As a example: the four cards at the top are the *key cards*, while the bottom card is one of 128 *responses cards*. Subject must associate one of four *key cards* to *the response card*. In our case, the association between *response card* and the first (1) *key card* is defined as "correct" if the rule is based upon the color similarity. After updating the rule to another similarity type (e.g., number of items), if the subject still associates *response card* to 1 *key card* (color feature), a perseverative errors is produced.